UC San Diego

UC San Diego Previously Published Works

Title

Piezoelectric rod sensors for scour detection and vortex-induced vibration monitoring

Permalink

https://escholarship.org/uc/item/2r80d7xh

Journal

Structural Health Monitoring, 21(3)

ISSN

1475-9217

Authors

Funderburk, Morgan L
Park, Yujin
Netchaev, Anton
et al.

Publication Date

2022-05-01

DOI

10.1177/14759217211018821

Peer reviewed

eScholarship.org Powered by the California Digital Library
University of California

Piezoelectric Rod Sensors for Scour Detection and Vortex-induced Vibration Monitoring

Morgan Funderburk[1,2], Yujin Park[2,3], Anton Netchaev[4], and Kenneth J. Loh[1,2,3,*]
[1]Department of Structural Engineering, University of California San Diego, La Jolla, CA 92093, USA;
[2]Active, Responsive, Multifunctional, and Ordered-materials Research (ARMOR) Laboratory, University of California San Diego, La Jolla, CA 92093, USA;
[3]Materials Science and Engineering Program, University of California San Diego, La Jolla, CA 92093, USA;
[4]U.S. Army Engineer Research and Development Center, U.S. Army Corps of Engineers, Vicksburg, MS 39180, USA

[*]E-mail : kenloh@ucsd.edu

ABSTRACT

As extreme events increase in frequency, flow-disrupting large-scale structures become ever more susceptible to collapse due to local scour effects. The objective of this study was to validate the functionality of passive, flow-excited scour sensors that can continue to operate during an extreme event. The scour sensors, or piezo-rods, feature continuous piezoelectric polymer strips embedded within and along the length of slender cylindrical rods, which could then be driven into soil where scour is expected. When scour erodes away foundation material to reveal a portion of the piezo-rod, ambient fluid flow excitations would cause the piezoelectric element to output a voltage response corresponding to the dynamic bending strains of the sensor. The voltage response is dependent on both the structural dynamic properties of the sensor and the excitation fluid's velocity. By monitoring both shedding frequency and flow velocity, the exposed length of the piezo-rod (or scour depth) can be calculated. Two series of experimental tests were conducted in this work: (1) the piezo-rod was driven into sediment around a mock pier to collect scour data and (2) the piezo-rod was used to monitor its own structural response by collecting vortex-shedding frequency data in response to varied flow velocities to establish a velocity-frequency (V-F) relationship. The results showed that the piezo-rod successfully captured structural vortex-shedding frequency comparable to state-of-practice testing. A one-dimensional numerical model was developed using the V-F relationship to increase the accuracy of voltage-based length prediction of the piezo-rod. Two-dimensional flow modeling was also performed for predicting localized velocities within a complex flow-field. These velocities, in conjunction with the V-F relationship, were used to greatly improve length-predictive capabilities.

Keywords: added mass, fluid-structure interaction, flow, frequency, monitoring, scour, soil, velocity

1. Introduction

Scour occurs when flowing water erodes streambed or bank material and is of particular concern when localized around hydraulic structures [1]. In particular, obstructions to normal flow, such as bridge piers, produce erosive vortices that cause significant displacement of sediments near the structure's base. Scour erosion can significantly undermine the stability of hydraulic structures and can lead to superstructure damage or catastrophic failure [2–4]. In the U.S., it is estimated that scour erosion of bridge foundations solitarily causes 20-100 collapses per year and causes similarly severe damage and losses worldwide [5,6].

Major flooding events rapidly exacerbate erosion levels, and, furthermore, scour can accumulate over multiple floods [4,5]. Damage to highways and bridges in the U.S. from major flooding events were estimated to cost roughly $100 million per event during an eight-year period [6]. Alternating periods of erosion and infill, particularly after flooding events, mean that surviving structures can be left with a compromised foundation system that appears undamaged [7]. In an unidentified vulnerable state, the superstructure may not survive another event, even of the same magnitude. Furthermore, increasing global temperatures, changing precipitation patterns, and alterations to the frequency and severity of flooding events exacerbate the problem of local scour [8,9]. The projected flooding risk brought by climate change is expected to increase the rate of hydraulic bridge collapse [10–12]. In some regions of the U.S., 90% of existing bridges would be vulnerable to scour in the next 75 years [13].

Very few viable monitoring techniques exist that are able to function during high-flow events when scour intensifies. Most of the existing techniques recommended by the Federal Highway Administration suffer from various drawbacks that make them unlikely to address the range of issues scour presents [1,14]. For instance, devices like sonar have difficulty functioning outside of still water conditions when entrained air and sediments hinder wave propagation, while those that do only have a limited coverage range [15]. Monitoring techniques that do function during extreme events, such as magnetic sliding collars, tilt sensors, float out devices, and robust time domain reflectometry (TDR), tend to be limited by either data quality or continuous functionality [16–18]. Recently, the predictive capabilities of TDR scour technology has improved, but functionality during high-flow events is yet to be verified [19].

In order to provide an uninterrupted stream of passively collected data, emerging techniques utilize the length-dependent structural properties of cantilevered rod-like sensors that can estimate the level of erosion based on vibrational feedback [14,20,21]. Azhari and Loh first proposed the design of a “piezo-rod scour” sensor, which was based on embedding a piezoelectric element in a long, slender rod. When scour exposes the buried piezo-rod, excitation from flowing water causes the piezoelectric element to output a voltage time history response. By decomposing the voltage time history to the frequency domain, the fundamental frequency of the system during a set time period was determined, which was correlated to its exposed length or scour depth. Others, such as Zarafshan *et al.* [21], developed a fiber Bragg grating (FBG) driven-rod sensor that also uses natural frequency to determine exposed length. However, fiber optic sensors and their data acquisition systems are costly, sensitive to temperature, and require fiber-optic cabling to be run to each sensor-rod. Furthermore, the FBG sensor is also placed at only one location along the length of the scour rod, making it more susceptible to irreparable damage. In contrast, the piezo-rod is designed with a piezoelectric element that runs along the entirety of its length and outputs voltage even when damage occurs on the free-end. In addition, the fact that piezo-rods do not require an external power source means that they can be more easily coupled with wireless data collection systems for long-term monitoring. Even so, all frequency-based scour sensors, whether piezoelectric- or FBG-based, must consider fluid flow effects, which impose complexities on the system that are not easily captured in closed-form equations.

In the context of piezo-rods, Funderburk *et al.* [14] applied various signal processing techniques to more reliably extract the fundamental frequencies from experimental piezo-rod voltage data but was not able to back-calculate scour depths (*i.e.*, exposed rod lengths). Results from this study showed that the frequencies increased over time, which was expected, but the back-calculated scour depths were not equal to the depths of scour that were observed during the experiments. Further testing revealed that the voltage response of piezo-rods was dependent on a link between the excitation fluid velocity and the vortex shedding frequency, herein referred to as the V-F relationship.

Previous determination of the V-F relationship required use of a special apparatus and experimentation in a highly controlled environment [22,23]. Therefore, this paper presents a novel method for determining the V-F relationship using solely a flowmeter and the piezo-rod, by exploiting the piezoelectric element. The V-F relationship was then included in the back-calculation of piezo-rod length using a unitless coefficient of

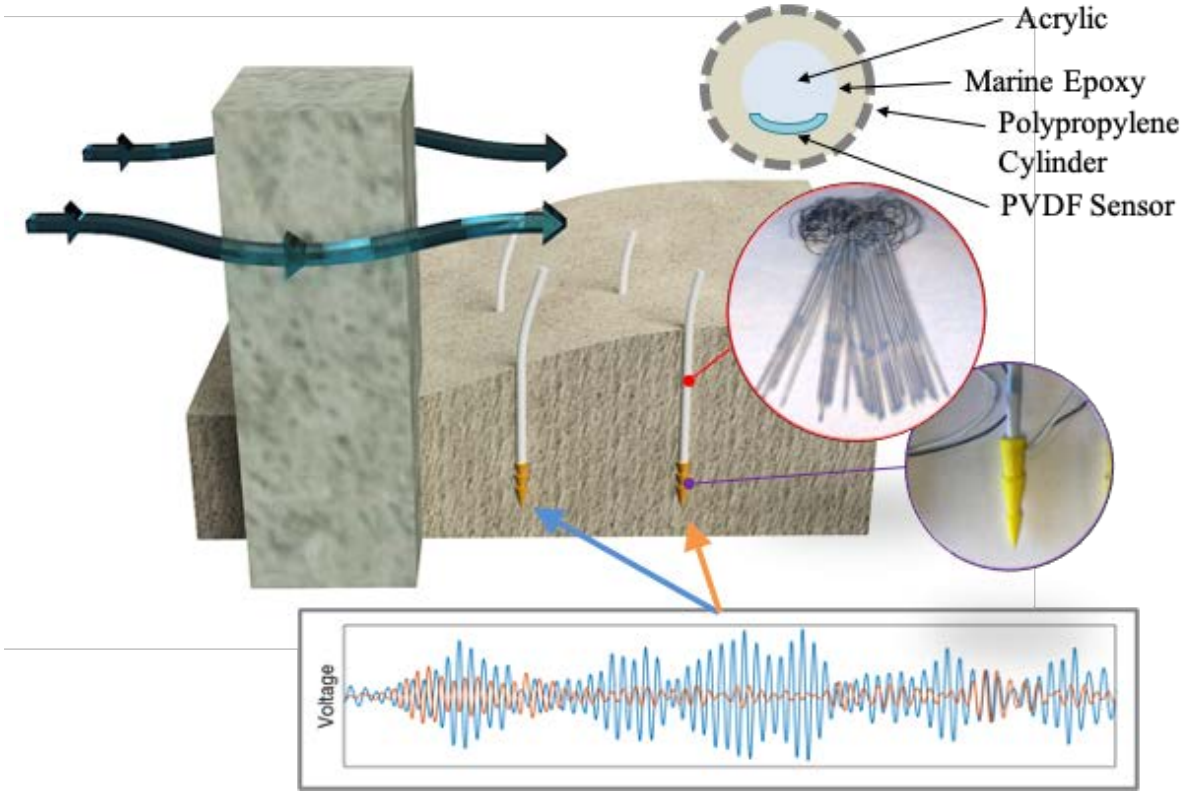

Figure 1: Vortex shedding during fluid-flow excites the piezo-rod sensors. The inset illustrates the cross-section of each piezo-rod sensor. Each sensor outputs a voltage corresponding to the rate of strain induced. As scour occurs, changes in the outputted frequency can be detected.

added mass (CAM) adjustment [22]. The CAM adjustment, along with two-dimensional (2-D) fluid-structure interaction modeling, improved the accuracy of piezo-rod length predictions in complex flow fields. The methodology proposed in this paper was then compared with other assumptions, which do not consider flow velocity effects, to verify the marked improvement in measuring scour depth.

2. Theory and Background

The piezo-rod sensors operate on the principle that the fundamental frequency of the sensor (which depends on multiple variables but most notably its length) can be used to back-calculate the exposed length or scour depth. When implemented *in situ*, the piezo-rods would be installed and buried vertically in the sediment surrounding a water-disrupting structural asset, such as a bridge pier (Fig. 1). During scour, any changes in sensor length would correspond to sediment movement during scour, either due to erosion or infill. By tracking the changes in the length of the sensor, the amount of scour in the immediate region of the sensor could be determined. Thus, a distributed network of these piezo-rods near a structural asset could allow one to determine the scour hole topography [14,24]. This section discusses a single-degree-of-freedom dynamic model of the piezo-rod while taking into consideration their use in fluid environments and soil boundary conditions.

2.1 Dynamic Analysis

The piezo-rod sensor can be modeled as an elastic cantilevered beam using Euler-Bernoulli beam theory, which excludes considerations for shear deformations and is the most commonly used beam model for high

aspect ratio structures [25]. Making the assumption that the cross-sectional area and elasticity are constant along the length of the beam and that there is no axial deformation, the homogenous equation of motion can be written as:

$$\frac{d^2}{dx^2}\left\{EI\frac{d^2y(x)}{dx^2}\right\} = 0 \tag{1}$$

where E is elastic modulus, I is moment of inertia, and $y(x)$ is the distance along the longitudinal axis of the beam or piezo-rod.

A single-degree-of-freedom system can be derived using Equation 1 and four boundary conditions corresponding to rotation and displacement perpendicular to the centerline of the beam. For simplicity, the starting assumption of the piezo-rod system is a fixed boundary on one end and a free boundary on the other. This yields a system with a mass, m, equivalent to the entire beam, and a structural stiffness of $k=3EI/L^3$. Thus, the fundamental frequency, f_n, is calculated to be:

$$f_n = \frac{1}{2\pi}\sqrt{\frac{k}{m}} \tag{2}$$

However, this assumption places the lumped mass of the beam entirely at the free end, which can lead to an underestimation of the structure's true natural frequency. Therefore, a more accurate value of the natural frequency of the beam system can be found by solving the differential equation describing a beam of distributed mass undergoing free-vibration [26]:

$$\frac{d^2}{dx^2}\left\{EI\frac{d^2y(x)}{dx^2}\right\} - \rho A y(x)\omega^2 = 0 \tag{3}$$

where ρ is density, A is cross-sectional area, and ω is angular frequency. The fundamental frequency can now be calculated using:

$$f_n = \frac{1.876^2}{2\pi L^2}\sqrt{\frac{EI}{\rho A}} \tag{4}$$

For the purposes of this study and future implementation of this system, it is more convenient to calculate frequency in the form of Equation 2, so an equivalent mass, $m_{eq}=33m/140$, was used. By substituting m_{eq} for the lumped-mass value, m, in Equation 2, the same fundamental frequency value is outputted as would be by the distributed-mass system in Equation 4. The ratio can be solved for by setting Equation 2 equal to Equation 4 ($m = \rho AL$). This equivalent mass and stiffness were used for frequency estimations of a fixed piezo-rod throughout the remainder of the study. When the sensor was submerged in still fluid, it was assumed that the weight of fluid is equivalent to the area displaced by the body[23]. The submerged mass of the sensor (*i.e.*, the sensor mass plus the displaced water mass) was then altered to be an equivalent distributed mass.

2.2 Spring-Pin Soil Boundary

A similar derivation of a single-degree-of-freedom system was used to incorporate a soil boundary condition seen during scour. The modeled soil boundary would replace the conventional fixed boundary with an approximate spring-pin system. The constrained end of the beam, $y(L)$, would be inhibited from movement perpendicular to the centerline and would only have moment resistance equivalent to the stiffness of a rotational spring. The value of the rotational soil spring, k_{ss}, was solved using a load-displacement (p-δ) test as demonstrated in Azhari and Loh [20]. The generalized value of the soil spring for

this system in loosely packed sand was 0.84 N/rad. To derive the lateral stiffness of the spring-pin system at the free-end, *y(0)*, the following boundary conditions were applied to Equation 1:

$$y(0) = 1,$$
$$EI\frac{d^2y(0)}{dx^2} = 0,$$
$$y(L) = 0,$$
$$EI\frac{d^2y(L)}{dx^2} = -k_{ss}\frac{dy(L)}{dx} \quad (5)$$

The new stiffness, k_{soil}, was calculated to be:

$$k_{soil} = \frac{3EIk_{ss}}{k_{ss}L^3+3EIL^2} \quad (6)$$

By substituting k_{soil} and m_{eq} into Equation 2 the complete system for calculating the fundamental frequency of a distributed mass system with a soil spring is given as:

$$f_n = \frac{1}{2\pi}\sqrt{\frac{k_{soil}}{m_{eq}}} \quad (7)$$

Equation 7 can then be used to solve for the fundamental frequency of a cantilever beam in soil, while minimizing error introduced when simplifying to a lumped-mass assumption for a truly distributed-mass beam and helps to minimize error in the one-degree-of-freedom frequency calculation when the moment-spring is applied.

3. Scour Testing

A series of laboratory scour tests were conducted using piezo-rod sensors and a scaled pier. A complete framework of these tests, as well as the processing techniques used to extract fundamental frequency, was explained detailed in Funderburk *et al.* [14]. However, this previous paper stopped short of back-calculating scour depth, which is the primary focus of this study. A summary of the relevant scour test will be outlined in this section. The frequency data extracted using Hilbert transform and wavelet packet transform in Funderburk *et al.* [14] from the square pier test series will be analyzed in depth using two different assumptions. In addition, with *a priori* knowledge of soil-spring stiffness and piezo-rod material properties, length of the exposed rod (due to scour) is the only unknown variable and can therefore be quickly solved from the piezo-rod's voltage time history data. Length values will be back-calculated using two separate fundamental frequency equations, which were presented in Sections 2.1 and 2.2, and compared.

3.1 Piezo-Rod Design

The 1.5 ft piezo-rod sensors were made of a 6 mm diameter polypropylene shell with an embedded polyvinylidene fluoride (PVDF) piezoelectric thin film element and infilled with marine epoxy (Fig. 1). It is well known that the piezoelectric element produces an electric field and corresponding voltage output in response to dynamic strains. When the piezo-rod is placed in flowing water, it acts as an obstruction to fluid flow, where vortex-induced vibrations (VIV) would strain the PVDF film to cause it to output a corresponding voltage response. The recorded voltage time history can then be converted to the frequency domain, where the dominant frequency of the signal corresponds to the natural frequency of the piezo-rod based on its structural properties and assumed boundary conditions.

The fabrication process began by injecting marine epoxy into the polypropylene shell. Then, a pre-wired PVDF film cut to a width of 4 mm (with metallized electrodes on opposite faces of the PVDF) was affixed onto an acrylic rod and inserted into the center of the filled shell. After hardening the marine epoxy, a 3-D printed cone footing was fitted onto one end of the piezo-rod to protect the wiring and to ease the insertion of the rod into soil during scour testing. A stair-stepped design was used on the cone footing to help prevent any movement or dislodging during testing.

3.2 Hydrodynamic Scour Testing

In this study, 11 piezo rods were driven around a pier into the loosely packed sand of a hydrodynamic flume's mobile bed zone. Piezo-rods were driven into sand by hand using only a small trowel to loosen sand in some areas. The sensors were not fixed in place and were only held upright by the surrounding soil. The face of the PVDF strip was placed orthogonal to the general direction of flow. The sensors were placed around one side of the base of a 6 cm square pier, since symmetry during scour hole formation was assumed (Fig. 2). The locations of the sensors were selected to best capture the expected scour hole topography.

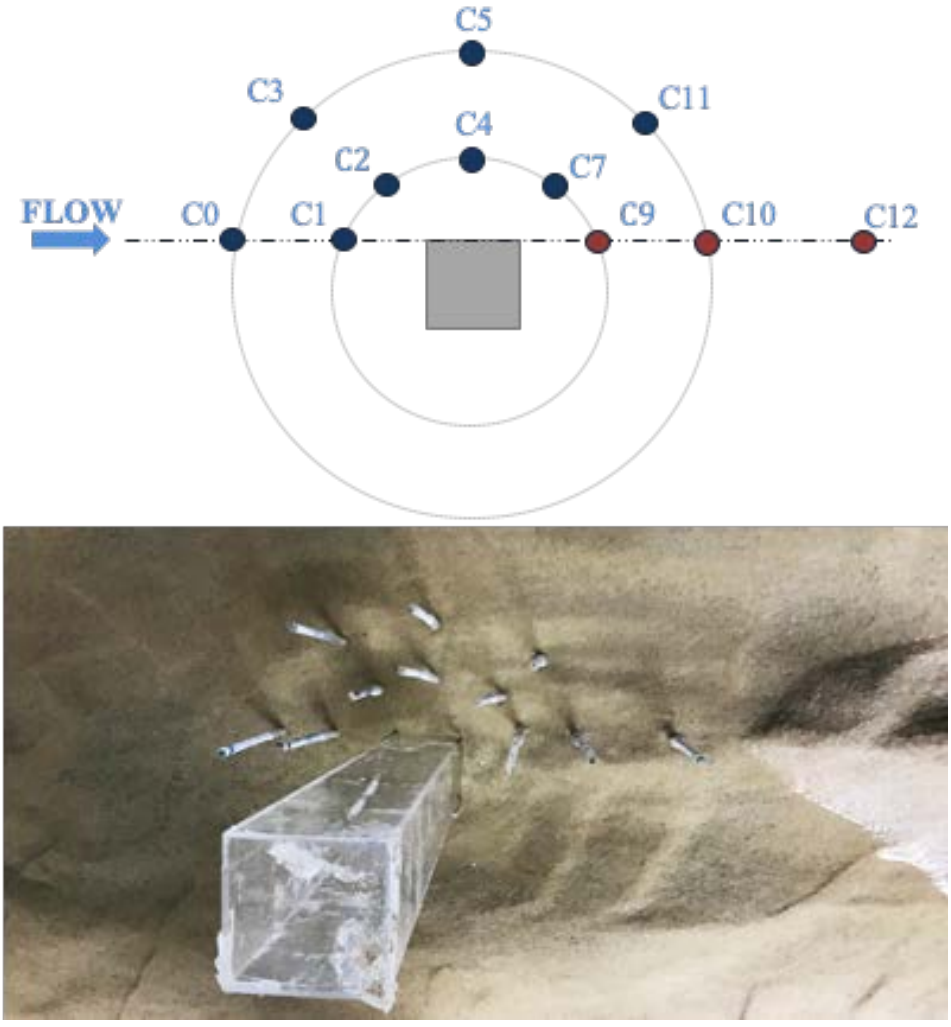

Figure 2: A total of 11 piezo-rod sensors were outfitted around a 6 cm square pier during scour experiments. The marked sensors (C9, C10, and C12) were removed from the results due to low excitation and therefore poor feedback.

When used as a set, the length feedbacks from each location would together produce a full scour hole topography surrounding the pier.

The sensor wires were buried near the pier and then kept close to the sidewall to avoid introducing unintended vortices into the testing zone. After the flume was filled with water, but before scour testing, the pre-flow length of the sensors was noted. During scour testing, three increasing levels of flow velocities were used to induce three degrees (or severities) of scour referred hereto forth as Low Scour, Medium Scour and High Scour. The three scour periods were introduced by controlling the volume of water flowing through the flume using a pump, which was adjusted based on its voltage and an exit ramp, adjusted based on its angle. The volume of water pushed into the flume and the rate at which water exited could be controlled through a combination of adjustments to the pump and exit ramp, thereby controlling flow velocity. During Low scour, the pump and exit ramp were set, based on previously established levels, to allow water to move through the flume at a sufficient rate to begin the scour process. The pump and gate were then adjusted, based on prior experience, to push more water through the flume for the Medium Scour period and then again for the High Scour period. The increase in scour during each flow period was confirmed visually, using measurement markings on the piezo-rods, before the flow velocity was increased. During the tests, flow velocity was measured with an acoustic Doppler velocimeter (ADV) and controlled by adjusting the flume's pump voltage and its outflow ramp. Each period of scour was recorded individually, but there was no break in flow between periods. Voltage data was recorded and digitized using a National Instruments DAQ PXIe-1062 chassis and PXIe-8133 controller equipped with a PXIe 4303, 32-channel, analog input module with 24-bit resolution and +/-10 V measurement range (sampling rate: 300 Hz). The DAQ and data storage was controlled manually using a customized program in LabVIEW. The lengths of each sensor were monitored visually and recorded before and after each scour period. These exposed lengths of the piezo-rods were assumed to be the ground truth and were used for comparison with piezo-rod post-processed results.

Water temperature has the potential to influence the stiffness of the material surrounding the piezo-element and therefore the natural frequency of the system. However, due to the controlled nature of this scour test, temperature changes were not considered. Temperature is not expected to influence the density of water where it would have a significant effect on response as it varies in density by only 0.008 g/cm^3 between 32 °F and 100 °F [27]. Furthermore, it should be noted that the impact of debris or physical damage to the sensor body once installed *in situ* would cause significant changes to the natural frequency, but debris effects are not considered in this study.

4. Structural Analysis

The post-processed piezo-rod exposed length results from the three periods of Low Scour, Medium Scour, and High Scour are shown from left to right, respectively, in Figures 3 and 4. The post-processed length results are shown as dots, while the observed visual piezo-rod lengths are shown with a darkened line. The observed visual length was collected by a team of observers, who manually recorded the exposed lengths by reading measurement markings on the piezo-rod. The thin dotted line represents the observed length before flow was initiated (*i.e.*, pre-flow). Black stars within each time window represent the average of the post-processed data for that scour period. This visualization will remain consistent in future figures. Differences in the average scour depth as determined by the piezo-rods and with respect to the visually observed levels of scour will be used to quantify the effectiveness of the proposed post-processing methods.

4.1 Fixed Boundary Conditions

Originally, it was assumed that a fixed boundary condition would be sufficient for estimating the piezo-rod's exposed length. In Figure 3, the piezo-rod data were post-processed assuming a fully fixed boundary

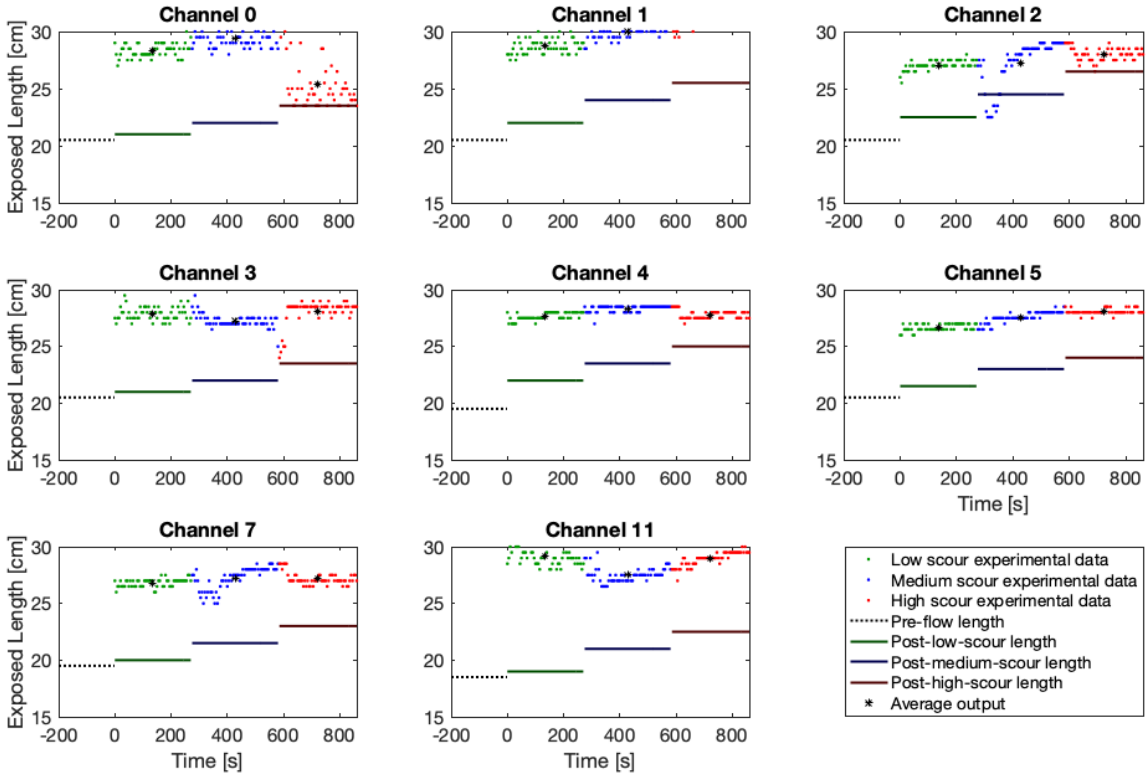

Figure 3: The piezo-rod data back-calculated using a fixed boundary assumption show a significant length over-estimation and inconsistent trends. The three scour periods Low (leftmost), Medium (center), and High (rightmost) are shown for each channel.

condition assumption. Prior to the scour test, each sensor was tested as a clamped cantilever in air to determine its elastic modulus. A composite assumption was used to estimate a singular density of the piezo-rods. The results of the fully fixed assumption are shown in Figure 3 and, as expected, indicate that the exposed length (or scour depth) output was a gross overestimation due to the various simplified assumptions.

4.2 Spring-Pin Results

Results after incorporating the spring-pin soil assumption are shown in Figure 4. The lengths determined using this new boundary condition now fall closer to the actual range observed during testing, particularly in the Low Scour period, when it is hypothesized that behavior would be most similar to still water conditions. This indicates that the spring-pin assumption was more situatable for modeling the complexities associated with soil-driven rods for this application. Still, both sets of results (Figs. 3 and 4) also indicate a shortening of the sensor during periods where no infill was noted. This phenomenon can be seen across all eight functioning channels in Figure 4 and is quite dramatic. On the other hand, three channels (namely, 9, 10, and 11) were excluded from the results due to the lack of flow excitation at those sensor locations, which led to a poor signal (and excitation) to noise ratio. Preliminary analysis of the data from these channels quickly revealed that the sensors were not experiencing sufficient excitation from vortex shedding, likely due to their positioning at the rear of the pier. The positioning of sensors will be discussed more in depth in section 6.

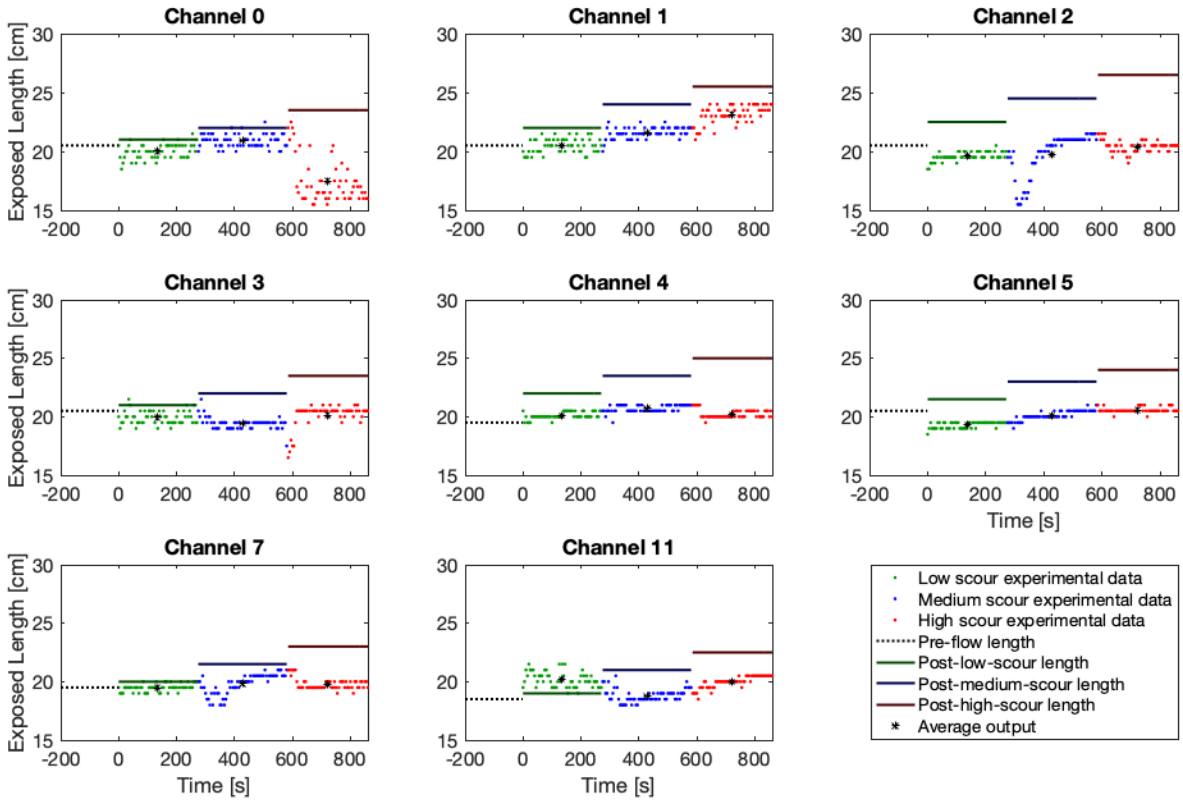

Figure 4: The piezo-rod data back-calculated using a pin-spring boundary condition show under-predicts the exposed length of each piezo-rod. The three scour periods Low (leftmost), Medium (center), and High (rightmost) are shown for each channel.

4.3 Justification for Flow Testing

Based on these initial results, it was determined that the effects of dynamically shifting flow velocities had more impact on the outputted piezo-rod frequency than determined in prior studies [14,20]. The necessity for quantifying a V-F relationship was likely overlooked during prior scour testing because flow velocity was kept constant during scour. With a constant velocity during scour testing, the V-F relationship was also relatively constant and could be accounted for within the range of structural parameters. Furthermore, minor changes to frequency output during prior V-F testing were not marked as significant by Azhari and Loh [20]. To develop a sufficiently accurate model of soil-driven scour rods, which relies on VIV fluid excitation, a method to account for the changes in distributed fluid mass in varied flow velocity is paramount and needed.

5. V-F Experiment

Two of the sensors used for scour testing were used to quantify the relationship between velocity and frequency. For this experiment, a triangular wooden truss was mounted to the base of a large concrete flume using bolts. The flume is 24 ft wide and can hold up to 10 ft of flowing water (Fig. 5a). The truss was designed as a right triangle to support two exposed piezo-rod sensors on the face, with the entirety of the truss placed downstream of the sensor (Fig. 5b). Two sensors were used simultaneously in order to collect more data during each test. The sensors were clamped with a free length exposed at the edge of a purposefully extended element facing the incoming flow (Fig. 5c). The reminder of the sensor was clamped

(a)

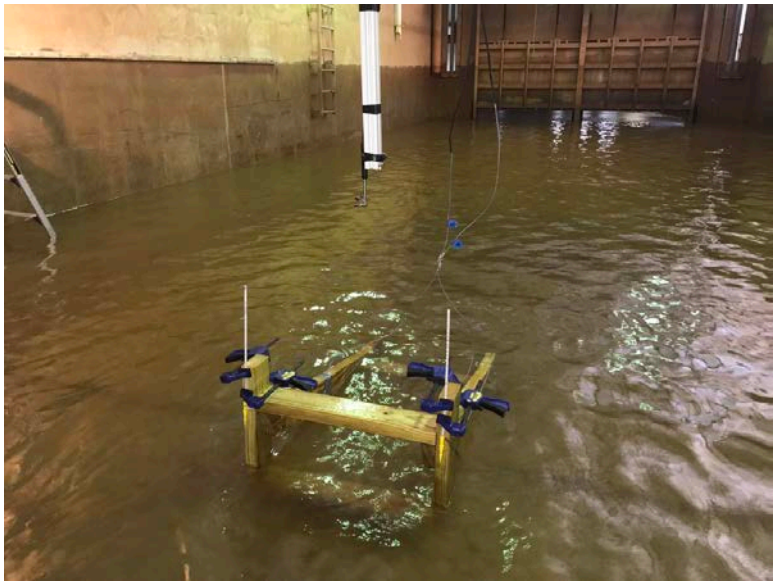

(b)

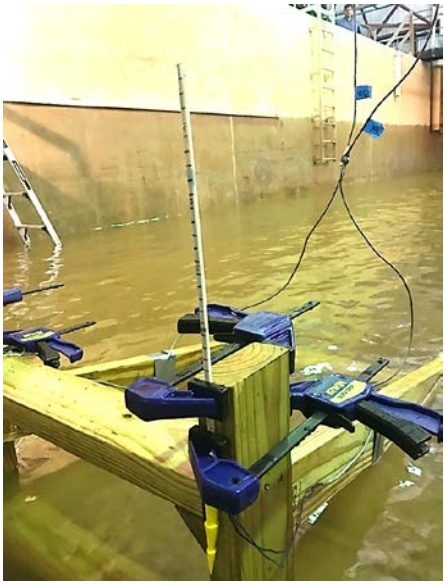

(c)

Figure 5: (a) The test specimen and supporting truss was bolted to the floor of a long concrete flume. (b) The piezo-rods were widely spaced and the ADV was placed both above and behind the piezo-rods, as not to disturb incoming flow. (c) The piezo-rods were clamped at the edge of the truss along the length below to prevent extraneous vibration.

further down the truss, to ensure that no vibrations occurred in the "fixed" portion. A test was also performed with a clamped sensor and no free portion of the piezo-rod exposed to ensure that the clamping method was sufficient in preventing vibration in the lower portion of the rod. The results, although not shown here, demonstrated that this method was suitable to mimic fully fixed piezo-rods of varying length.

The piezo-rods were conservatively spaced ~100 times their diameter apart and at the same height so as to not affect the other piezo-rods' vibrations. The acceptability of piezo-rod spacing was determined based on numerical simulations and secondarily by the observable wake during testing. An ADV was placed slightly downstream and above the tip of the exposed piezo-rod, visibly upstream of the wake crossing point behind

the two piezo-rods (Fig. 5b). The flume was designed specifically for lock-and-dam testing and therefore had a unique system for circulating water. The circulation, and therefore bulk flow, of water was controlled by a series of four pumps and a large gate which lifted incrementally and allowed water to flow beneath it into the reserve basin. The velocity was limited by the pump capacity, the volume of water contained in the basin, and height of water needed in the testing area.

The dimensions of the flume were 20 ft (6 m) wide, 120 ft (36.5 m) long, and up to 12 ft (3.5 m) deep, although realistically only 10 ft (3 m) of water could be circulated faster than 10 cm/s. The complete test setup required 4.5 ft (1.5 m) of water in order to fully submerge the velocimeter. Imperfections existed along the floor of the flume, so the supporting structure was built with enough height so that the clamped edge of each piezo-rod was at least ~2 ft off the base of the flume to avoid disrupted fluid flow. The piezo-rods were placed halfway down the length of the flume and downstream from outflow due to vortices created upstream by the pump. Fluid-flow was relatively smooth in this region, as recorded by the ADV. Visibility in the water was poor, but the increase in suspended sediment improved the ADV's functionality.

5.1 Testing Protocol

Piezo-rods were fixed at 2 cm increments ranging from 20 cm to 28 cm, representing approximately the lengths seen during scour testing. After fixing the sensors to the desired length, the flume was filled using the smallest pump until the water level reached 4.5 ft or 1.5 m. The flume was put through a predetermined series of pump engagements and gate lifts in an effort to increase fluid flow incrementally while keeping the height of water in the flume constant. The exact procedure for changing these variables was decided prior to placement of the piezo-rods and was followed closely for each test. Although the velocity increased over time, it was not as steady or repeatable as desired.

5.2 Data Acquisition Protocol

The piezo-rods' wires were attached to the rear of the truss and brought out of the water downstream of the test setup, then looped around a catwalk spanning the width of the flume. The direct wiring to the piezo-rod was of a copper wire twisted pair. The twisted pair is necessary for fabrication but was cut short and welded to a coaxial BNC cable to shield the voltage signal from electronic noise. All submerged connections were coated in two layers of epoxy to prevent water breach. The BNC cables were run along the catwalk and into a control room where they were connected to a National Instruments data acquisition (NI DAQ) PXIe-1062 chassis and PXIe-8133 controller equipped with a PXIe-4303, 32-channel, analog input module card with 24-bit resolution and ±10 V voltage range (sampling rate: 300 Hz). The differential leads were grounded to the NI DAQ using resistors to stop the signal from floating. DAQ control and data storage was performed using a customized LabVIEW program.

5.3 Results and CAM Adjustment

The Strouhal number (St) is a well-known relationship between the value of periodic vortex shedding behind a cylindrical body and the immersed freestream velocity. The St relationship to frequency is given as [28]:

$$St = \frac{f_s D}{U} \tag{8}$$

where f_s is the shedding frequency, U is the fluid velocity, and D is the hydraulic diameter. An St of 0.2 was assumed for the piezo-rod, which is well known to be acceptable for a cylinder over a wide range of Reynolds numbers.

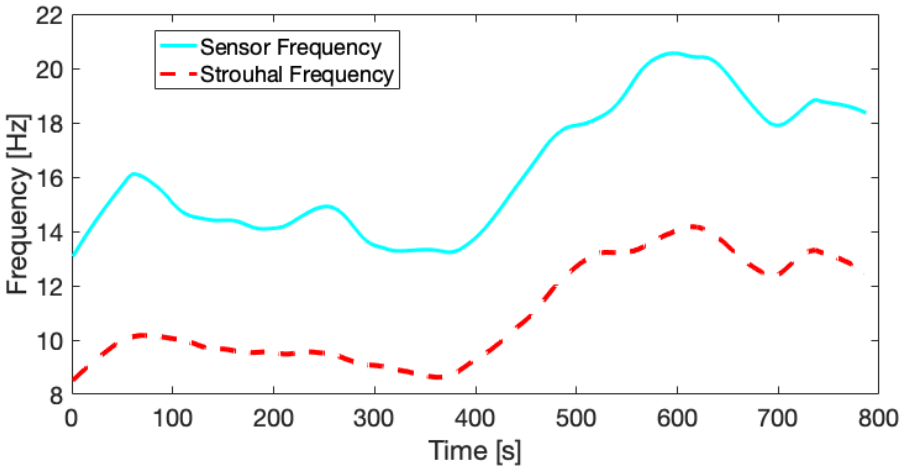

Figure 6: The outputted frequency of the sensor does not match but corresponds well with the Strouhal frequency, which is directly related to flow velocity.

Voltage time history data from the piezo-rods was processed using a bandpass filter, Hilbert transform, and smoothed using a least squares (LSQ) regression with weighted outliers in MATLAB. The frequency data was averaged to contain the same number of points as the ADV data, which sampled significantly slower and at 25 Hz. Figure 6 shows the expected Strouhal frequency calculated from the ADV data as compared with the instantaneous frequencies extracted from the voltage data. It can be clearly seen that, while the two datasets follow similar trends, the Strouhal frequency does not govern the piezo-rods' response due to the fixed boundary condition at one end.

An aggregate of the relevant data was used to produce a normalized relationship, which could be used to post-process piezo-rod data at a range of flow velocities, following experimentation seen in Vikestad *et al.* [22]. The frequency was normalized using an equivalent coefficient of added mass, which was calculated using the fully fixed structural model by minimizing the error between the outputted frequency and the model from Equation 2. The CAM was used to adjust only the added mass of the fluid and was found to be between -0.6 and 0.6 in this experiment, although the upper limit approached infinity while the lower limit appeared asymptotic (Fig. 7a). Velocity data was normalized into a set of reduced velocities, U_r, using the relationship:

$$U_r = \frac{U}{D f_{nw}} \tag{9}$$

where f_{nw} is the submerged natural frequency in still water.

CAM adjustment was then fitted with a lower boundary LSQ second degree polynomial curve, as this would eventually lead to a slight overestimation of lengths given the spread of data. The raw voltage data was also examined to look for the presence of lock-in. In Figure 7b, the maximum voltage output from each averaged time window is plotted with respect to the reduced velocity for the 20 cm exposed length case, where a pronounced peak is apparent around a reduced velocity of 2. However, it was observed that this peak largely disappeared as the length increased past 24 cm, and large excitation was seen at a variety of velocities. The initial results suggested that the maximum voltage is a sufficient parameter determining the relative level of excitation of a body (corresponding to the amplitude of oscillation).

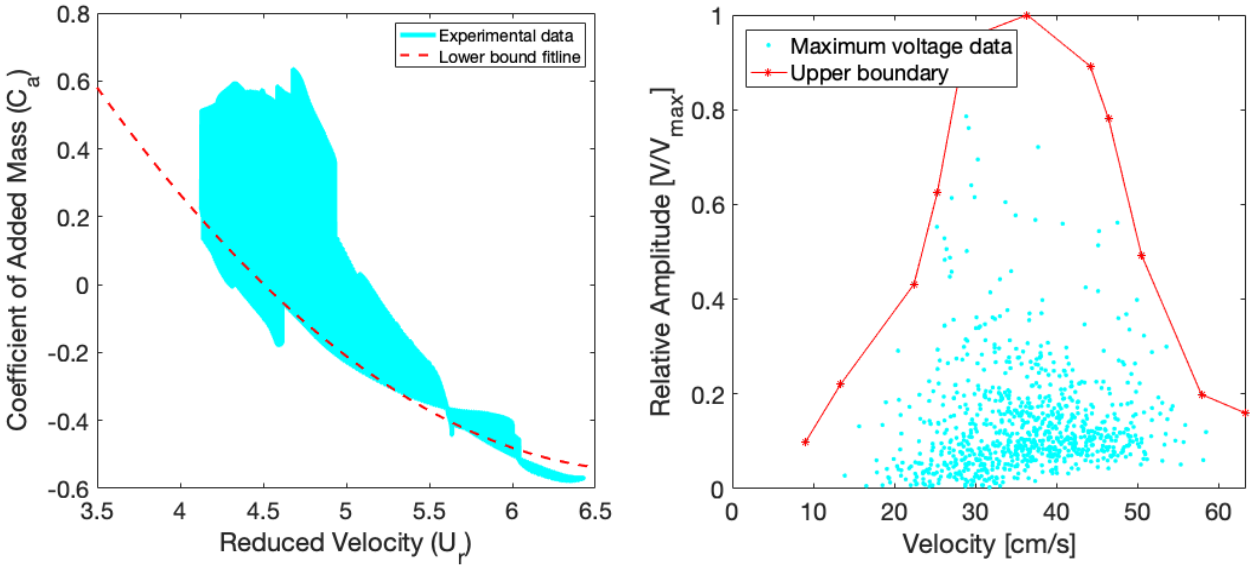

(a) (b)

Figure 7: (a) Based on V-F experimentation, the coefficient of added mass is plotted against the reduced velocity exciting the system. (b) The maximum voltage output is representative of the relative amplitude of excitation. The maximum voltage output is plotted versus velocity, and the boundary of this relationship is shown.

6. 2-D Fluid-Structure Interaction Modeling

A two-dimensional fluid-structure interaction model was developed in COMSOL to further understanding of piezo-rod placement and response. This model had the secondary aim of capturing localized velocity effects experienced by each sensor during scour testing. A 2-D model is preferred due the computational and time expense associated with 3-D fluid modeling.

6.1 Model Parameters

The flume used by Funderburk *et al.* [14] was drawn to its specification, meaning that the fluid-flow area was the same width and length used during experimentation (Fig. 8). An inlet specifying maximum velocity was placed at one end of the flume with a zero-pressure outlet at its opposite end. A moving mesh was applied surrounding the cross-sections representing the piezo-rods. The square pier incorporated in the model was chosen to be a fixed rigid body, while the piezo-rods were modeled using their material properties. The piezo-rod cross-section was fixed with springs in the *x*- and *y*-directions and allowed to oscillate.

Numerical probes were placed in both the *x*- and *y*- directions to capture the displacement of the body at each time step. Figure 9 shows a one-second sample window of the *y*-direction displacement (*i.e.*, perpendicular to flow) of the piezo-rod cross-sections after flow began. An iterative model study showed that adjusting the stiffness of springs had no effect on the final vibration frequency. This is because the two-dimensional model assumes that the cross-section is a rigid-body cylinder, which sheds vortices governed by the Strouhal equation (Equation 8). An inlet specifying maximum parabolic approximation was used based on the central location of the ADV during scour testing. Large Eddy Simulation Regularized Based Variational Multiscale (LES RBVM) turbulence was employed. Flow velocities ranging from 15 cm/s to 45 cm/s were run, which encompassed the entire range of the scour tests.

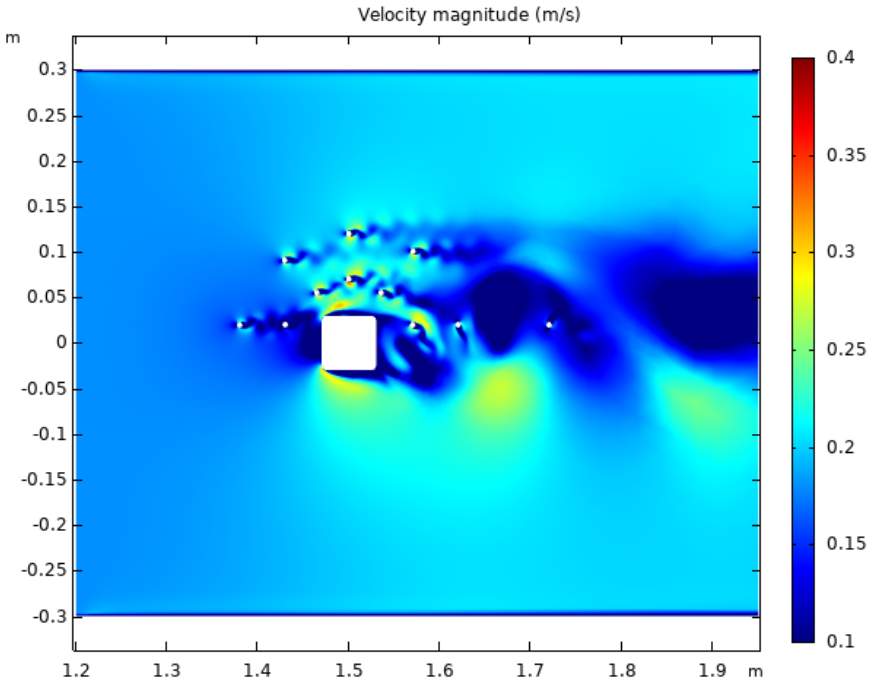
Velocity magnitude (m/s)
m
0.3
0.25
0.2
0.15
0.1
0.05
0
-0.05
-0.1
-0.15
-0.2
-0.25
-0.3
1.2
1.3
1.4
1.5
1.6
1.7
1.8
1.9
m
0.4
0.35
0.3
0.25
0.2
0.15
0.1

(a)

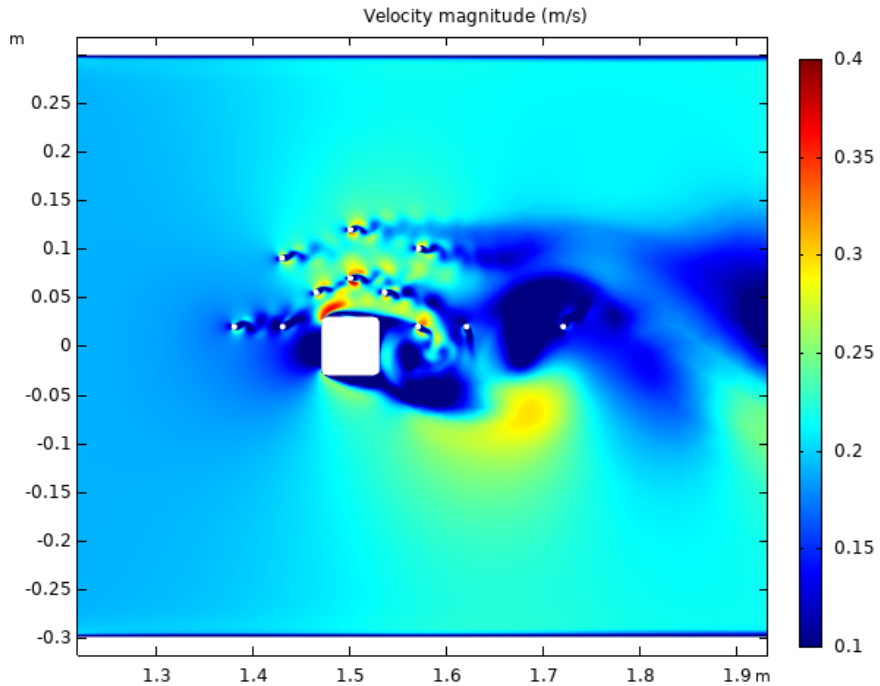
Velocity magnitude (m/s)
m
0.25
0.2
0.15
0.1
0.05
0
-0.05
-0.1
-0.15
-0.2
-0.25
-0.3
1.3
1.4
1.5
1.6
1.7
1.8
1.9
m
0.4
0.35
0.3
0.25
0.2
0.15
0.1

(b)

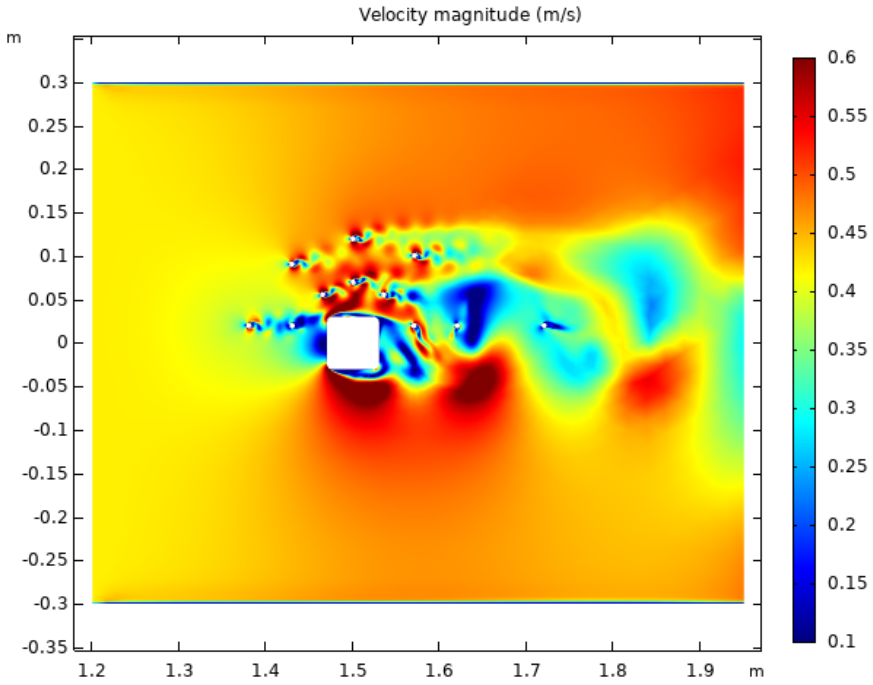

(c)

Figure 8: Results from the 2-D fluid-structure interaction COMSOL model were used to quantify the magnitude of velocity experienced by each channel in the flow field during the (a) Low, (b) Medium, and (c) High Scour periods.

6.2 Localized Velocity using Strouhal Number (St)

The frequency of each sensor perpendicular to flow was extracted from a simple Fourier decomposition of the probe plots. An St of 0.2 was assumed, and the VIV driving velocity for each sensor was calculated. Three increasing levels of velocities were evaluated to account for the periods of Low Scour, Medium Scour, and High Scour (Fig. 8). The individualized velocity extracted for each piezo-rod from this model was then used as an input for the length calculation with CAM adjustment. Notably, however, a 2-D assumption cannot capture any vortices that may occur due to scour hole formation, which undoubtedly play some role in the overall piezo-rod excitation.

The displacement time history response of piezo-rods in the rear (*i.e.*, channels 9, 10, and 12) confirms their relatively low levels of excitation and therefore freestream velocities. As seen in Figure 10, the piezo-rods in the rear did not experience the same magnitudes of flow velocity versus those in the front and side of the pier. The low level of excitation seen during scour testing is therefore explained by placement behind a substantial obstruction in the flow-field. However, the low level of excitation in the rear does not hamper the capability of the piezo-rod to collect sufficient scour data.

Typically, the most critical location for scour occurs at the face of the pier, where downflow initially displaces soil and allows erosive horseshoe vortices to form. The piezo-rods function well along the front and side of the pier, where flow is more consistent. Further downstream from the pier, where smooth flow is restored, piezo-rods can be used detect infill. The combination of depth measurements from the front and side topography, as well as information about downstream infill, provides a greater scope of topographic information than other anchored near-pier scour sensing systems. Even with the inability to function in locations where flow is obstructed, the piezo-rods are a useful tool for scour

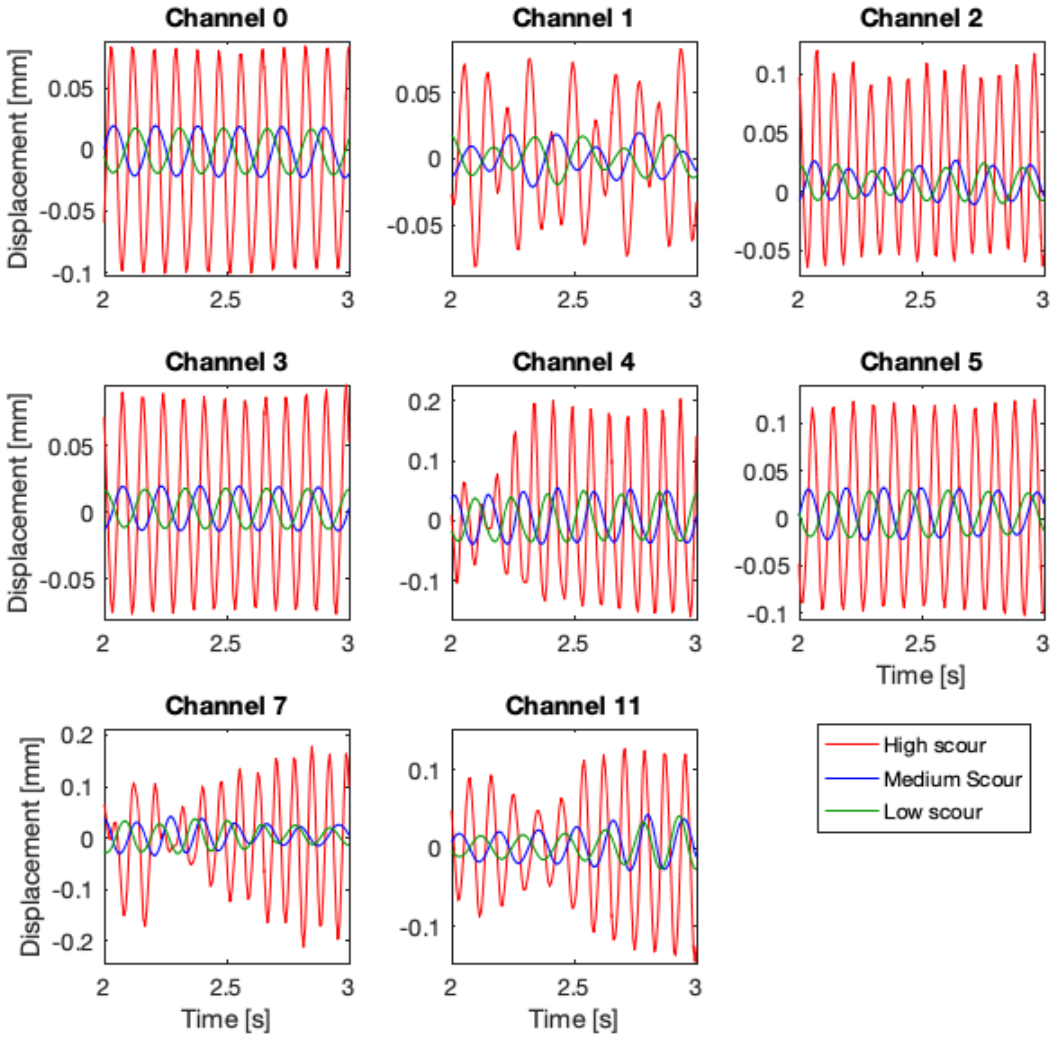

Figure 9: The displacement time history of each piezo-rod sensor in the direction perpendicular to flow during the Low, Medium, and High Scour periods are plotted, and the results were used to calculate localized velocity.

monitoring during extreme events, and can fill in the current gaps in capability left by current scour technologies, particularly in regards to topographic sensing during high or murky water flow conditions. Furthermore, the use of the piezo-rods can be readily used to detect scour away from piers (*i.e.*, open water or abutment) without the added concern of zero-flow pockets. The piezo-rods present a great advantage for use in scour locations in which an over-water structure is not available for anchorage.

7. Scour Results with CAM Adjustment and Localized Velocity

The final results of this study were processed using three main amendments to the fixed cantilevered beam approach, namely, by incorporating a spring-pin soil assumption, a lower-boundary LSQ CAM adjustment fit line, and localized velocity results obtained from a 2-D fluid-structure interaction model (Fig. 11). As shown in Figure 11, improvements in the average length levels are seen across all channels, where it

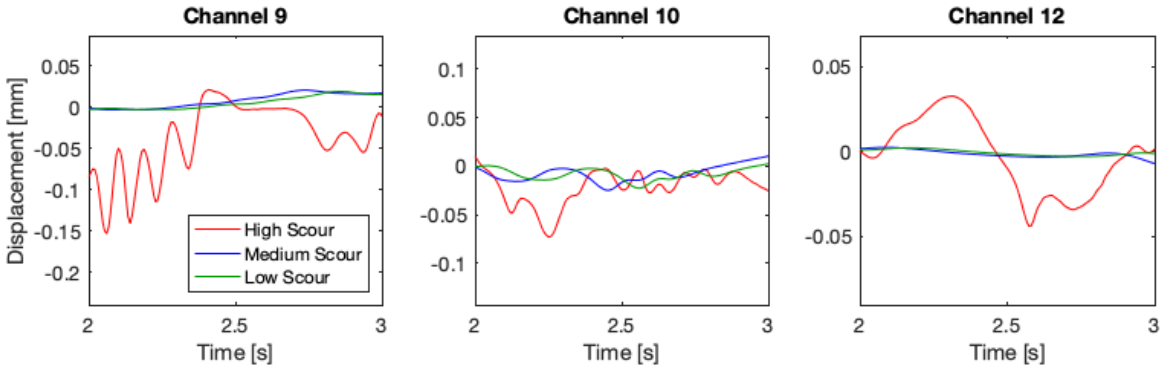

Figure 10: Displacement perpendicular to flow is shown during the Low, Medium, and High Scour periods at locations corresponding to the low response channels. Channels showing relatively poor oscillation response in the COMSOL model were consistent with the channels that showed poor response during the scour experiments.

approaches the observed results (*i.e.*, assumed ground truths). An increase in length, and therefore increase in scour hole depth, was observed as scour progressed from Low to Medium to High. This contrasts with previous iterations that incorrectly showed either constant or decreasing levels of scour. A comparison of the three methods shown in this study is presented in Table 1, and it is clear that the aforementioned enhancements for processing piezo-rod data can improve scour depth estimation accuracy. For comparison purposes, an average length error metric will be used that uses the difference between the observed length, L_{true}, and length calculated from each modeling method, L_{calc}, given as:

$$Length\ Error = \frac{1}{n}\sum_{i=1}^{n} \left|L_{true,i} - L_{calc,i}\right| \tag{9}$$

where n is equal to the number of channels (in this case there were nine). The standard deviation of the Length Error for each scour period was also calculated.

Results from Table 1 show that by using only a fixed condition, length estimation is particularly poor in the Low and Medium scour periods. This is due to an overestimation in the expected support provided by the soil, where vibration is present in the sensor system below the surface while appearing to have a shorter functional length. Once the soil is accounted for with the soil-spring assumption lengths in the Low and Medium Scour periods improve significantly, but the High Scour period remains elusively poor. This

Table 1: Mean length errors (LE) and their standard deviations (SD) of error between observed and calculated piezo-rod exposed lengths based on different modeling methods

	Length Error [cm]					
	Low Scour		Medium Scour		High Scour	
	LE	SD	LE	SD	LE	SD
Fixed	6.7	1.7	5.4	1.4	4.0	1.8
Soil Spring	1.5	0.8	2.5	1.1	4.0	1.5
CAM-Soil Spring	1.1	0.8	1.3	0.9	1.9	1.3

Note: The mean length error was computed as an absolute value and does not account for difference between under and over estimation of length.

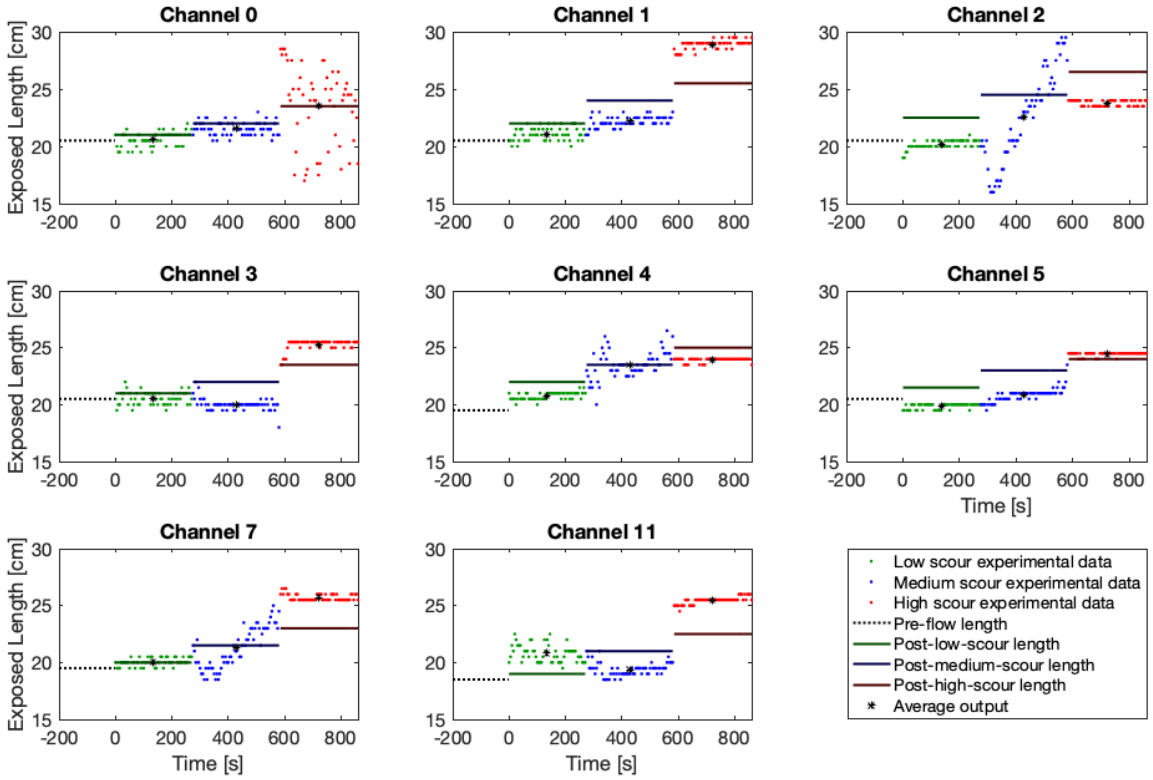

Figure 11: The piezo-rod data back-calculated using a pin-spring boundary condition and CAM adjustment show the expected "stair-stepped" data that were also in the range of the experimentally measured exposed lengths after each scour period. The three scour periods Low (leftmost), Medium (center), and High (rightmost) are shown for each channel.

discrepancy matches the hypothesis that the increasing level of velocity during these three scour periods plays an increasingly significant role in their frequency output; the High Scour period is concurrent with the highest velocity period, where a lack of accounting for the velocity effect would be most apparent. With the introduction of the CAM adjustment, it can be seen that the error and the standard deviation of error are reduced in all three scour periods.

Even with use of the CAM adjustment, overestimation of lengths by about 3 cm is apparent in the High Scour regions, particularly in the channels corresponding the side of the pier (Fig. 11). This suggests that these sensors were experiencing higher velocities during the final scour period than estimated by numerical simulations. Other variances in the data are attributed to local vortices unaccounted for in the 2-D FSI model or from turbidity introduced by the flume pumps or flume imperfections. This local velocity phenomenon is hypothesized to present itself in data as dips and peaks in otherwise steady length prediction. Nevertheless, any variance in sensor behavior from the mathematical model would appear more significant due to the small-scale of this experiment. It is expected that these errors would be significantly reduced in a full-scale implementation of piezo-rods in the field.

8. Conclusions

This study demonstrated an enhanced processing scheme for improving the accuracy of scour depth measurements from data collected using prototype piezoelectric driven-rod scour sensors excited by vortex

shedding. Initially, as determined by previous studies, a spring-pin soil assumption was included to increase the accuracy of an oversimplified fully-fixed assumption. However, the inclusion of the soil-spring did not remove the unusual instances of mismatch between the observed increase in depth of the scour hole and the calculated decrease in depth of the scour hole. This discrepancy was seen when using both the fully-fixed and soil-spring assumption to back-calculate the outputted frequencies.

To correct these discrepancies in the final calculation, localized velocity effects near each piezo-rod, which were obtained from a 2-D fluid-structure interaction model, were newly incorporated using the CAM adjustment to account for dynamically shifting fluid velocity. Calibration of the added mass effect due to VIV excitation was shown to be successfully quantified using the novel approach of decomposing voltage time histories collected from the piezo-rod. When these methods were used for processing piezo-rod data obtained during hydraulic scour tests, the results clearly showed that scour depths could be accurately and reliably determined.

Compared with widely used scour monitoring techniques, the piezo-rod was designed particularly to function during extreme events when entrained air and muddy water impede other measurement types. As a system, the piezo-rods can give a topographic map of the scour damage (rather than just one location), and because they are passive, have the potential to function wirelessly without contributing to battery drain. The piezo-rods also have the distinct advantage of being able to function without an over water structure, such as a bridge, which allows them to cover a larger geographical region or monitor scour in open water.

Future studies will focus on demonstrating the scalability of the scour monitoring technology by testing and modeling large-scale (6 ft) piezo-rods. For the longevity and overall success of field implementation, studies are also needed to identify and quantify debris impacts. The authors hypothesize that structural health monitoring methods can be used to identify changes from impact and damage in the rod through the evaluation of signatures in the voltage time history. Other environmental changes that have the potential to effect frequency, such as temperature, should also be considered in the future. If a temperature measurement is taken at the installation site, thermal effects on the piezo-rod's material properties can likely be accounted for within the length prediction model.

Acknowledgements

This research was supported by the U.S. Army Corps of Engineers (USACE) Cooperative Research Agreement No. W912HZ-17-2-0024. The authors acknowledge Dr. A. Drew Barnett and Dr. Joseph Reed from Elintrix, as well as Prof. Michael Todd and Prof. Chin-Hsiung Loh from UC San Diego, for their collaboration and assistance with various aspects of this project. The authors gratefully acknowledge the staff of engineers and technicians at the U.S. Army Engineer Research and Development Center (ERDC) who assisted with the large undertaking of flume operation and test apparatus construction for the V-F testing. The authors also gratefully acknowledge the Department of Civil Engineering at the National Taiwan University for allowing the use of their hydraulic flume (Director: Prof. H. Capart), as well as Dr. Shieh-Kung Huang, Mr. Wei-Jay Ni, Ms. Tsai-Jung Kuo, Mr. Chuan-Fu Li, Ms. Yu-Xin Wu, and Mr. I-No Yu for their assistance with scour testing and data collection.

Disclosure of Conflicts

The authors declare no conflicts of interest.

References

1. U.S. Department of Transportation, Federal Highway Administration. *Bridge Scour and Stream*

Instability Countermeasures: Experience, Selection, and Design Guidance. 2009.
2. Stein BSM, Young GK, Trent RE, et al. Prioritizing Scour Vulernable Bridges Using Risk. *J Infrastruct Syst* 1999; 5: 95–101.
3. Bolduc LC, Gardoni P, Briaud JL. Probability of exceedance estimates for scour depth around bridge piers. *J Geotech Geoenvironmental Eng* 2008; 134: 175–184.
4. American Association of State Highway and Transportation Officals. *AASHTO LRFD Bridge Design Specifications*. 2010.
5. Flint MM, Fringer O, Billington SL, et al. Historical analysis of hydraulic bridge collapses in the continental United States. *J Infrastruct Syst*; 23. Epub ahead of print 2017. DOI: 10.1061/(ASCE)IS.1943-555X.0000354.
6. Pizarro, Manfreda, Tubaldi. The Science behind Scour at Bridge Foundations: A Review. *Water* 2020; 12: 374.
7. Richardson EV, Richardson JR. *Bridge Scour*, https://mountainscholar.org/handle/10217/80405 (1989).
8. Prein AF, Rasmussen RM, Ikeda K, et al. The future intensification of hourly precipitation extremes. *Nat Clim Chang* 2017; 7: 48–52.
9. Khelifa A, Garrow LA, Higgins MJ, et al. Impacts of climate change on scour-vulnerable bridges: Assessment based on HYRISK. *J Infrastruct Syst* 2013; 19: 138–146.
10. Wright L, Chinowsky P, Strzepek K, et al. Estimated effects of climate change on flood vulnerability of U.S. bridges. *Mitig Adapt Strateg Glob Chang* 2012; 17: 939–955.
11. Meyer MD, Weigel B. Climate Change and Transportation Engineering: Preparing for a Sustainable Future. *J Transp Eng* 2011; 137: 393–403.
12. Nasr A, Kjellström E, Björnsson I, et al. Bridges in a changing climate: a study of the potential impacts of climate change on bridges and their possible adaptations. *Struct Infrastruct Eng* 2019; 0: 1–12.
13. Neumann JE, Price J, Chinowsky P, et al. Climate change risks to US infrastructure: impacts on roads, bridges, coastal development, and urban drainage. *Clim Change* 2015; 131: 97–109.
14. Funderburk ML, Huang S-K, Loh C-H, et al. Densely distributed and real-time scour hole monitoring using piezoelectric rod sensors. *Adv Struct Eng* 2019; 22: 3395–3411.
15. De Falco F, Mele R. The monitoring of bridges for scour by sonar and sedimetri. *NDT E Int* 2002; 35: 117–123.
16. Yao C, Darby C, Hurlebaus S, et al. Scour monitoring development for two bridges in Texas. *Geotech Spec Publ* 2010; 958–967.
17. Richardson JR, Price GR, Richardson EV, et al. *Modular magnetic scour monitoring device and method for using the same*. 5,532,687, United States: U.S. Patent and Trademark Office., 1996.
18. Yankielun NE, Zabilansky L. LABORATORY INVESTIGATION OF TIME-DOMAIN REFLECTOMETRY SYSTEM FOR MONITORING BRIDGE SCOUR. 1999; 125: 1279–1284.
19. Wang K, Lin CP, Chung CC. A bundled time domain reflectometry-based sensing cable for monitoring of bridge scour. *Struct Control Heal Monit* 2019; 26: 1–14.
20. Azhari F, Loh KJ. Laboratory validation of buried piezoelectric scour sensing rods. *Struct Control Heal Monit* 2017; 24: 1–14.
21. Zarafshan A, Iranmanesh A, Ansari F. Vibration-based method and sensor for monitoring of bridge scour. *J Bridg Eng* 2012; 17: 829–838.
22. Vikestad K, Larsen CM, Vandiver JK. Experimental Study of Excited Circular Cylinder in Current. In: *International conference on offshore mechanics and arctic engineering. American Society of Mechanical Engineers*. 1997, pp. 231–240.
23. Vandiver JK. Dimensionless parameters important to the prediction of vortex-induced vibration of long, flexible cylinders in ocean currents. *Journal of Fluids and Structures* 1993; 7: 423–455.
24. Azhari F, Scheel PJ, Loh KJ. Monitoring bridge scour using dissolved oxygen probes. *Struct Monit Maint* 2015; 2: 145–164.
25. Bauchau OA, Craig JI. Euler-Bernoulli beam theory. In: Bauchau OA, Craig JI (eds) *Structural*

Analysis. Dordrecht: Springer Netherlands, pp. 173–221.
26. Meirovitch L. *Analytical Methods in Vibrations*. First Edit. New York City, NY: Macmillan, 1967.
27. Bureau of Reclamation United States. *Ground water manual: a guide for the investigation, development, and management of ground-water resources*. 1977.
28. Chen S-S. *Flow-induced vibration of circular cylindrical structures*. Argonne, IL (United States), 1985.